Electronic Supplementary Material (ESI) for Nanoscale.

Cost-Effective Carbon Fiber Precursor Selections of Polyacrylonitrile-Derived Blend Polymers: Carbonization Chemistry and Structural Characterizations

Qian Mao[1], Siavash Rajabpour[2], Mahdi Khajeh Talkhoncheh[2], Jiadeng Zhu[3], Malgorzata Kowalik[1], Adri C.T. van Duin[1,2,*]

[1]Department of Mechanical Engineering, The Pennsylvania State University, University Park, PA, 16802, United States

[2]Department of Chemical Engineering, The Pennsylvania State University, University Park, PA, 16802, United States

[3]Chemical Sciences Division, Oak Ridge National Laboratory, Oak Ridge, TN, 37831, United States

*Corresponding authors. Emails: acv13@psu.edu (Adri C. T. van Duin)

Section S1. Data Postprocessing Details

The conversion ratio of C atoms to 5, 6, 7-membered all-carbon rings in **Figure 2**, **Section 3.1** was computed by taking the number of C atoms constructing 5, 6, 7-membered all-carbon rings divided by the total number of C atoms from each precursor. Since one C atom may constitute multiple all-carbon rings, the summation of the conversion ratios of 5, 6, 7-membered all-carbon rings could exceed 1.0. On the other hand, the ratio $R_{\frac{6-MR}{5-MR\,\&\,7-MR}}$ in **Figure S3** (c), **Section 3.1** was computed by taking the number of 6-membered all-carbon rings divided by the total number of 5- and 7-membered all-carbon rings present in each given system.

The percentages of O- and N-containing species in **Figure 3** (a-d), **Section 3.2** were computed by taking the numbers of O- and N-containing gases or functional groups divided by the total numbers of O and N atoms in systems, multiplying by 100 %. The ratios of the remaining O- and N-containing species at 2250 ps in **Figure 3** (e-f), **Section 3.2** were calculated by taking the numbers of O- and N-containing gases or functional groups divided by the total numbers of C atoms from the clusters containing 3 to 8-membered all-carbon rings. The mass percentages of CH_4, CO, CO_2, H_2, H_2O, N_2, NH_3 in **Figure S4**, **Section 3.2** were computed by taking the molecular weights of these gas molecules divided by the molecular weight of each precursor, multiplying by 100 %.

The conversion percentages of C atoms in the basal plane or on the edges of turbostratic graphene, O atoms to O-containing groups, and N atoms to N-containing groups in **Figure 4** (a), (c), (e), **Section 3.2** were calculated by taking the numbers of basal plane or edge C atoms, O-containing groups, and N-containing groups divided by the total numbers of C atoms, O atoms, and N atoms in each systems, multiplying by 100 %, respectively. The ratios of C atoms, O atoms, and N atoms in **Figure 4** (b), (d), (f), **Section 3.2** were computed by taking the numbers of the given types of atoms divided by the numbers of C atoms constituting 3 to 8-membered all-carbon rings at 2250ps. The schematics of the occurrence of C atoms in the basal plane or on the edges of turbostratic graphene, the O-containing groups including carbonyl groups, hydroxyl groups, and C-O-C bridge bonds, and the N-containing groups comprising nitrile groups, imine groups, pyridine-like groups, amine groups, and graphitic-N groups can be found in our previous paper[34].

The graphitic C conversion ratios in the form of 3 to 8-membered and 6-membered all-carbon rings in **Figure 5** (a-b), **Section 3.3** were calculated by taking the numbers of C atoms from PAN or from the blended polymers that constitute 3 to 8-membered and 6-membered all-carbon rings divided by the total number of C atoms in each considered system.

The carbon contents in percentage in **Figure S5** (g), **Section S2** were calculated by taking the masses of C atoms from the biggest clusters of oxidized PAN carbonized at 2200 K, 2500 K and 2800 K at 8250 ps divided by the total masses of the remaining materials in each considered system, multiplying by 100 %. The conversion ratios of 5, 6, 7-membered all-carbon rings in **Figure S5** (h), **Section S2** were computed by taking the numbers of C atoms constructing 5, 6, 7-membered all-carbon rings divided by the total numbers of C atoms of oxidized PAN carbonized at 2200 K, 2500 K and 2800 K at 8250 ps.

The carbon contents in percentage in **Figure 6** (a), **Section 3.4** were derived by taking the masses of C atoms from the biggest clusters of each representative precursor divided by the total masses of the remaining materials at 2250 ps, multiplying by 100 %. the conversion of turbostratic graphene in percentage in **Figure 6** (b), **Section 3.4** was computed by taking the number of C atoms from the biggest cluster of each representative precursor divided by the total number of C atoms in the system at 2250 ps, multiplying by 100 %.

The first method for plotting the sp^2 C ratios in **Figure 8** (i), **Section 3.4** defines a C atom as an sp^2 hybridized C as its coordination number is 3, which only 3 neighbor C atoms are directly bonded with the target C. The second method[73] for plotting the perfect sp^2 C ratios in **Figure 8** (j), **Section 3.4** was to identify a C atom as an sp^2 hybridized C atom if (a) it only has 3 neighbor C atoms that all belong to the 6-membered all-carbon rings; (b) the distance, d, between the target C atom and the plane formed by the 3 neighbor C atoms meets $d < 0.5$ Å; (c) the C atoms on the edges of graphitic networks yet is directly connected with the C atoms identified by (a) and (b) are also counted. Then, the sp^2 C ratios of these two methods were computed by taking the numbers of sp^2 C atoms divided by the total numbers of C atoms from each representative precursor.

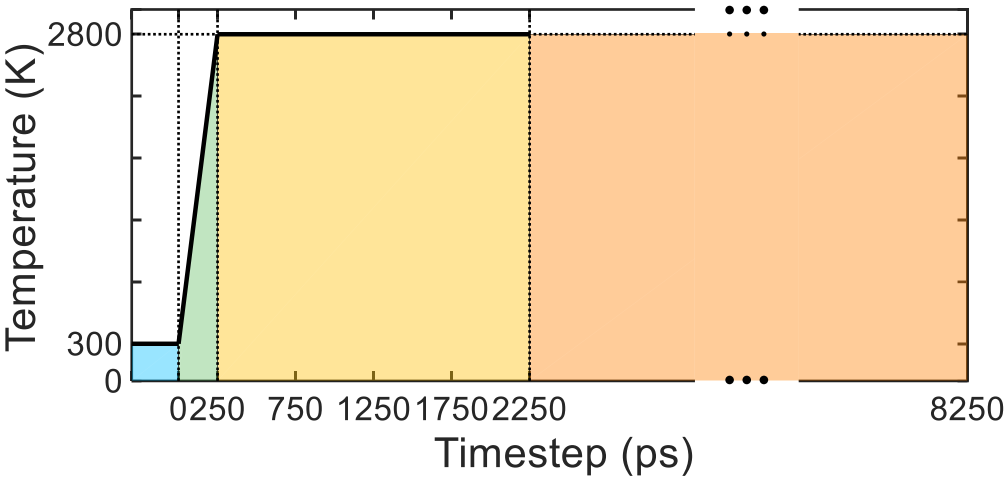

Figure S1. The schematic of thermal treatments for all considered single and blend precursors: The blue region is the equilibration process at 300 K for 300ps-1000ps; The green region is the heating process from 300 K to 2800 K with a heating rate of 10 K/ps over 250ps; The yellow regime is the carbonization process at 2800 K for 2000ps, and the orange regime stands for the extended carbonization process for the representative precursors of interest. We count the time from the beginning of the heating process (t = 0ps) to the end of the carbonization process (t = 2250ps for all cases, and t = 8250ps for the representative cases).

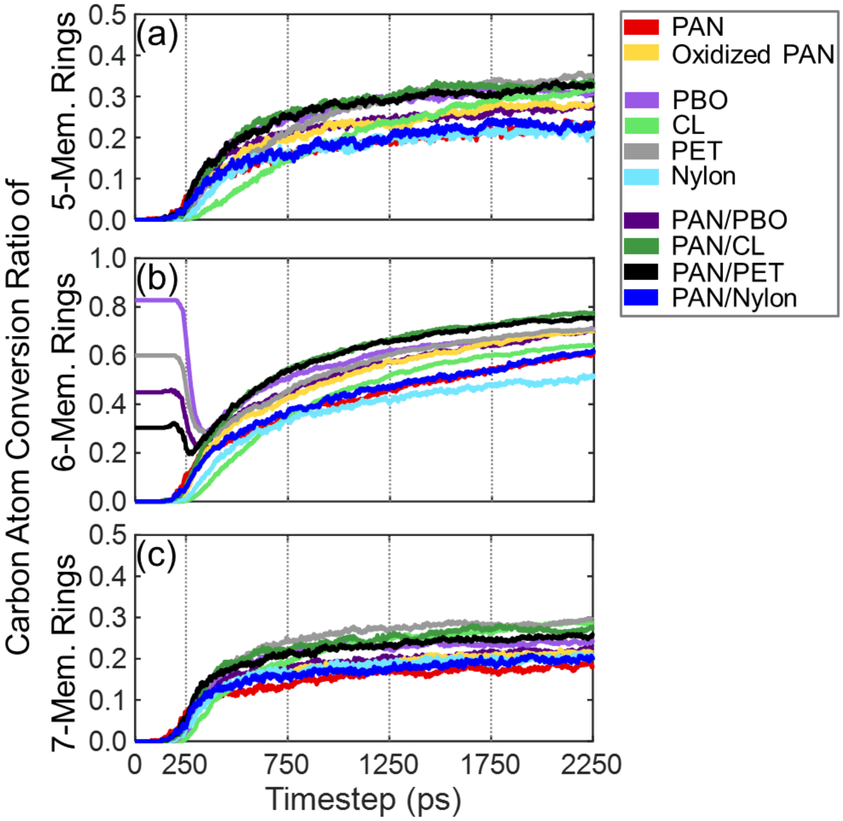

Figure S2. The normalized ratios of all-carbon rings for all considered single and blend precursors: (a) 5-membered, (b) 6-memebred, and (c) 7-membered all-carbon rings during the heating and carbonization processes (from t = 0ps to t = 2250ps). The normalization of 5/6/7-membered all-carbon rings is derived by taking the number of C atoms constructing the 5/6/7-membered all-carbon rings divided by the total number of C atoms from each precursor.

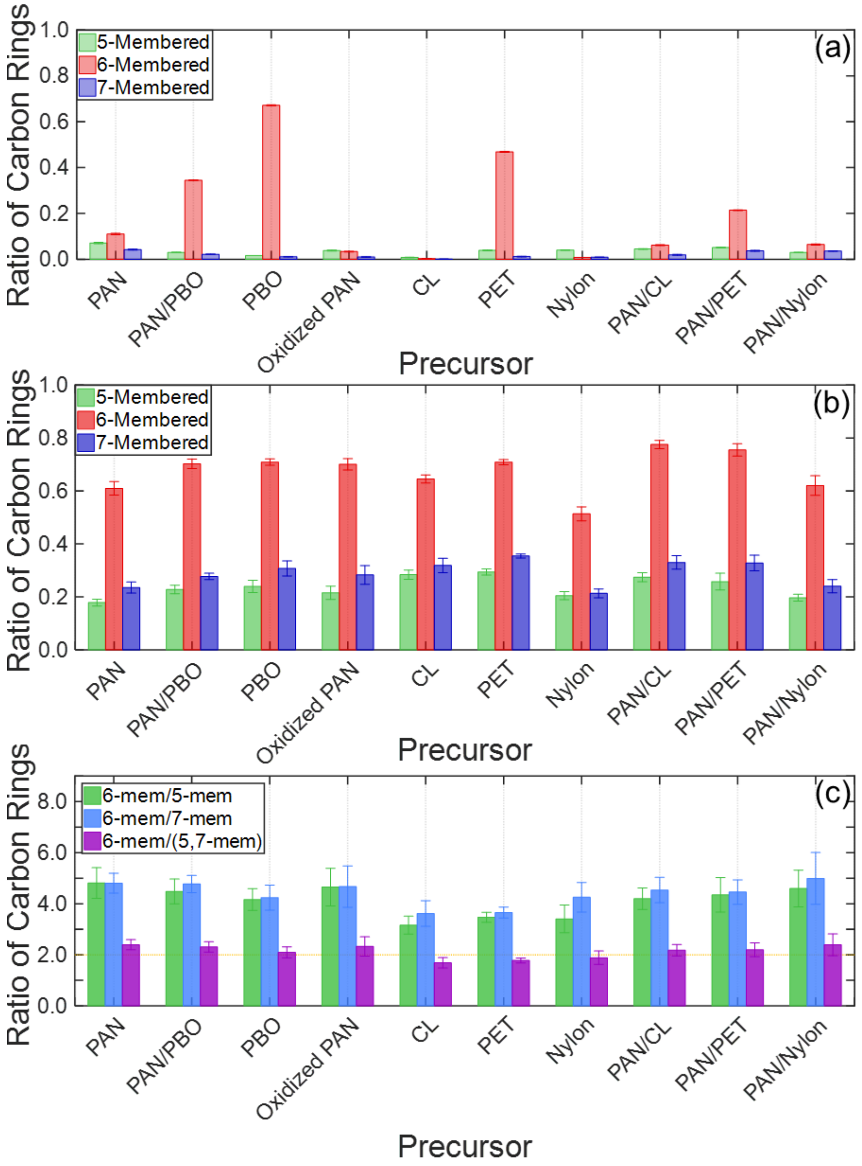

Figure S3. The normalized ratios of all-carbon rings for all considered single and blend precursors (a) in the beginning (t = 250ps) and (b) at the end (t = 2250ps) of the carbonization process. (c) The ratios of 6-membered to 5-membered all-carbon rings, 6-membered to 7-membered all-carbon rings, and 6-membered to 5- and 7-memebered all-carbon rings at the end of carbonization process (t = 2250ps). The error bars represent the standard deviations by 6 samples for each case. (a) and (b) are computed by taking the number of C atoms constructing 5/6/7-membered all-carbon rings divided by the total number of C atoms from each precursor, and the ratios in (c) are computed by taking the number of 5/6/7-membered all-carbon rings in the division.

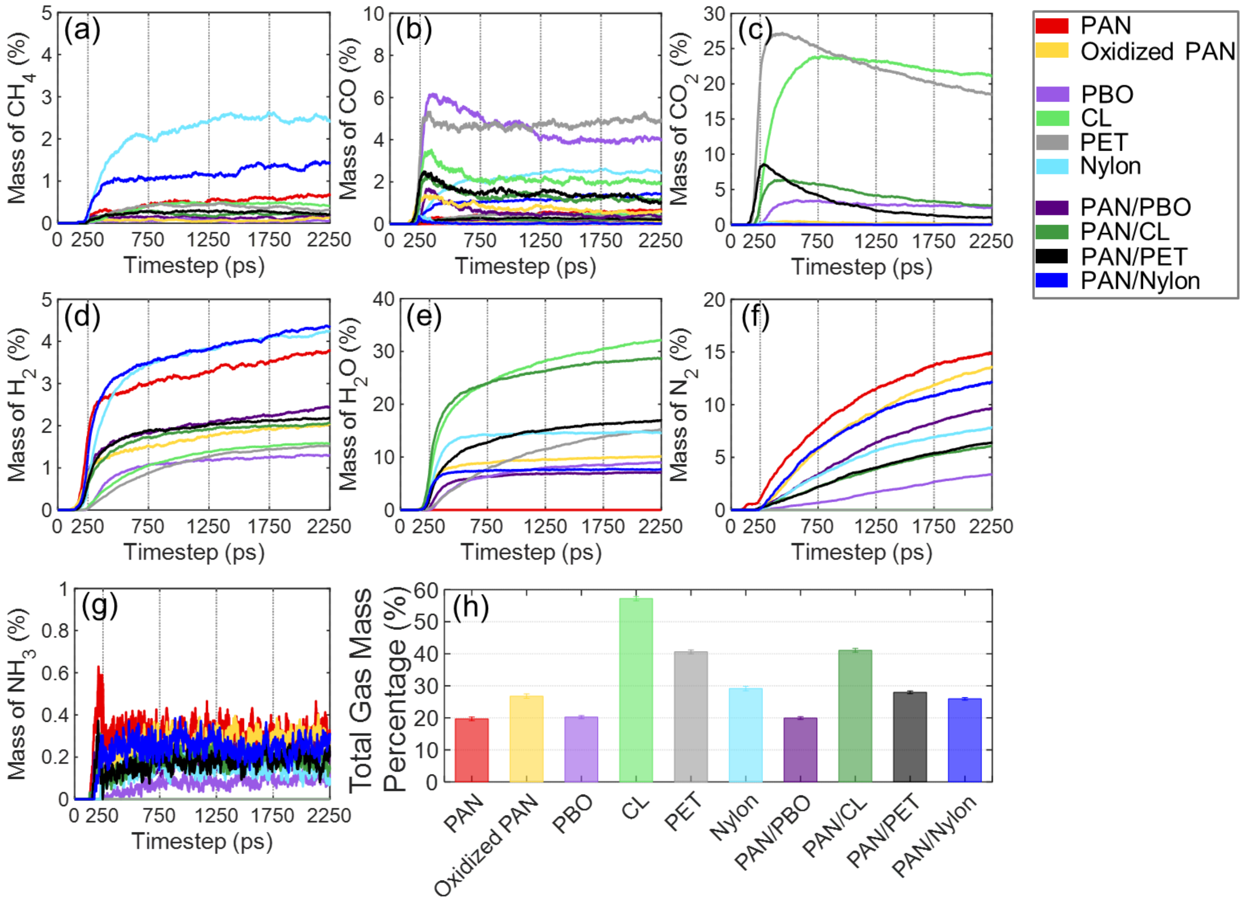

Figure S4. The evolutions of mass percentages of various volatile gases: (a) CH_4, (b) CO, (c) CO_2, (d) H_2, (e) H_2O, (f) N_2, (g) NH_3. The total gas mass percentage for all considered pure and blend precursors at the end of the carbonization process (t = 2250ps) is shown in (h). The curves are plotted by the mean values averaged from 6 samples. The error bars represent the standard deviations by 6 samples for each case.

Table S1. The total gas mass percentages and hetero element mass percentages for the ten single and blend precursors.

Precursor	**Total Gas Mass Percentage (%)**	**Hetero Element Mass Percentage (%)**
PAN	19.69	31.94
Oxidized PAN	26.75	37.04
PBO	20.23	27.95
CL	57.23	56.16
PET	40.61	37.63
Nylon	29.16	35.76
PAN/PBO	19.93	29.84
PAN/CL	41.09	46.56
PAN/PET	27.98	34.94
PAN/Nylon	25.92	33.93

Section S2. Morphological Variations of Carbonized Oxidized PAN from Experiment and ReaxFF Simulations

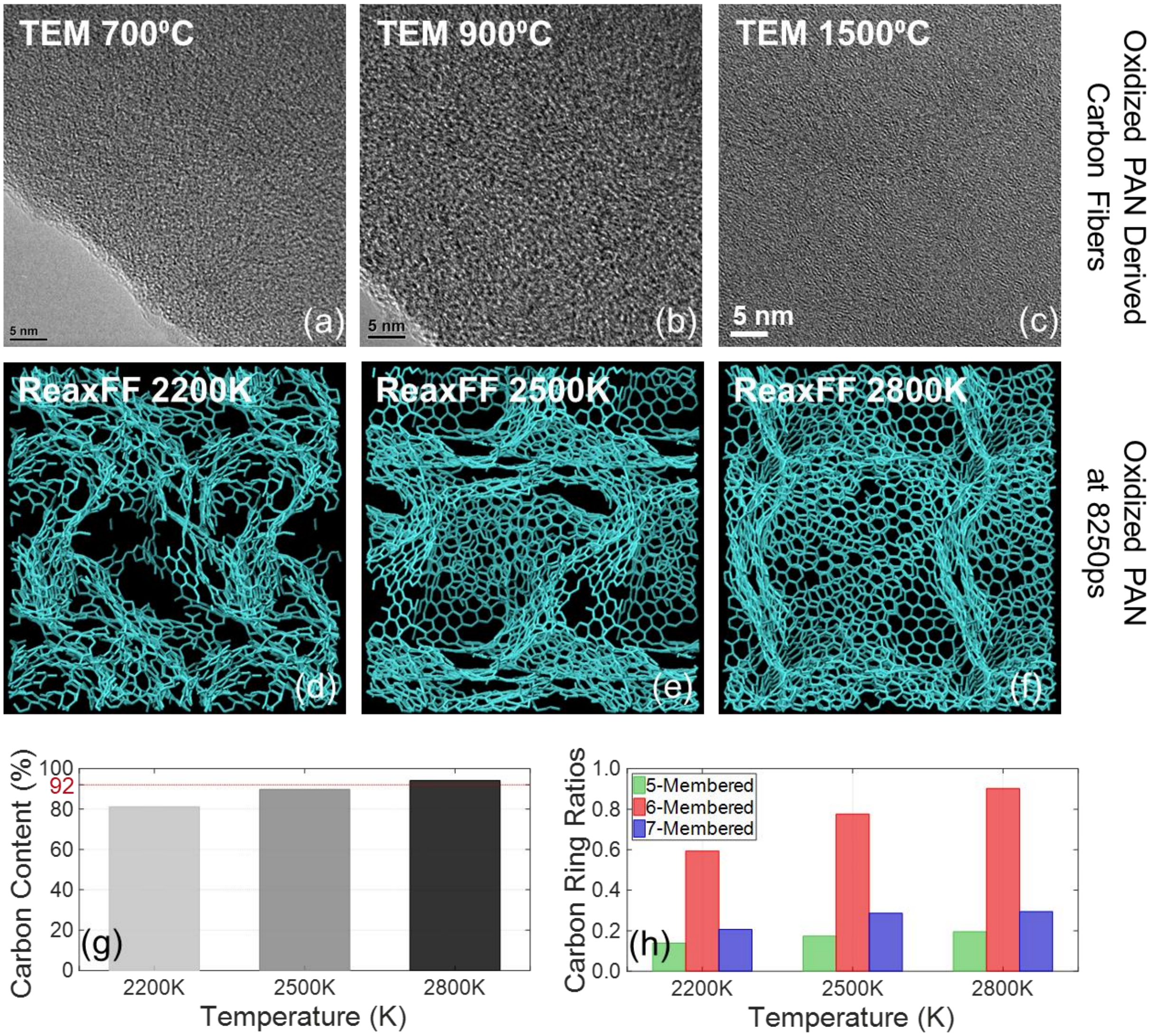

Figure S5. The comparison between the experimental TEM images and the ReaxFF MD snapshots of oxidized PAN precursor, for the characterization of all-carbon ring structure formation in response to elevated temperatures: The TEM images of oxidized PAN carbonized at (a) 700 ºC, (b) 900 ºC, and (c) 1500 ºC; The ReaxFF MD snapshots of oxidized PAN carbonized at (d) 2200 K, (e) 2500 K, and (f) 2800 K. The quantitative studies of all-carbon ring structure formation of oxidized PAN at elevated temperatures from ReaxFF MD simulations are also presented: (g) the carbon contents in percentage at 2200 K, 2500 K, and 2800 K; (h) the ratios of 5, 6, 7-membered all carbon rings at 2200 K, 2500 K, and 2800 K. The ReaxFF MD snapshots shown in (d) - (f) are mapped with the periodic boundary condition. The ReaxFF MD snapshots and bar plots are acquired after 8000 ps of carbonization, where the all-carbon ring structures are substantially developed.

We aim to demonstrate the feasibility of ReaxFF C/H/O/N-2019 simulating the turbostratic and graphitic structures for precursor samples undergoing carbonization, thus, we select and simulate oxidized PAN samples carbonized at elevated temperatures. Subsequently, we compare the morphological variations from computations with the experimental measurements.

Figure S5 (a-c) show the HR-TEM images of the oxidized PAN carbonized at 700 ^oC, 900 ^oC, and 1500 ^oC. There is no major difference between the samples carbonized at 700 ^oC and 900 ^oC, and both of them indicate amorphous structures, which is probably due to their relatively low carbonization temperatures[75,76]. However, for the sample carbonized at 1500 ^oC, the aligned-layer structures can be clearly observed in **Figure S5** (c), indicating the remarkable effects of carbonization temperatures on structure development of CFs. Since the estimated simulation time for oxidized PAN reaching 95 % carbon conversion to 6-membered all-carbon rings at 2800 K was identified to be ~7000 ps[34], here we apply the extended carbonization time (orange region in **Figure S1**) for oxidized PAN and then extract the carbon networks at 8250 ps and at 2200 K, 2500 K, and 2800 K. In **Figure S5** (d), the carbon structures display small all-carbon ring clusters and amorphous carbon residues woven together at 2200 K. As temperature goes up to 2500 K, the disordered structures begin to merge in the form of turbostratic graphene sheets, as can be notably seen in **Figure S5** (e). The graphene sheets stack layer by layer, and the larger porous structures start to develop. At 2800 K, the open carbon rings observed at 2500 K are closed, forming larger well-connected and layered structures, and the extensive all-carbon ring networks of higher crystallinity can be seen in **Figure S5** (f). As such, since the all-carbon ring formation and the turbostratic graphene network growth of oxidized PAN from the simulations are in line with the experimental trend identified by the TEM images, we believe that our ReaxFF simulations can reasonably predict the morphological evolutions of the selected precursors during the carbonization and graphitization processes.

Furthermore, we quantify the formation of all-carbon rings at elevated temperatures by carbon contents and the ratios of 5, 6, 7-membered all-carbon rings. As can been seen in **Figure S5** (g), the carbon contents at 2200 K, 2500 K, and 2800 K all exceed 80 %, while the carbon content at 2800 K is over 92 %, reaching the grade of manufacturing CFs[77]. The ratios of 5, 6, 7-membered all-carbon rings at these three temperatures are depicted in **Figure S5** (h). The higher ratio of 6-membered all-carbon rings can be observed at a higher temperature. Whereas there is no significant increase of 5 and 7-membered all-carbon rings as the temperature rises from 2500 K to 2800 K.

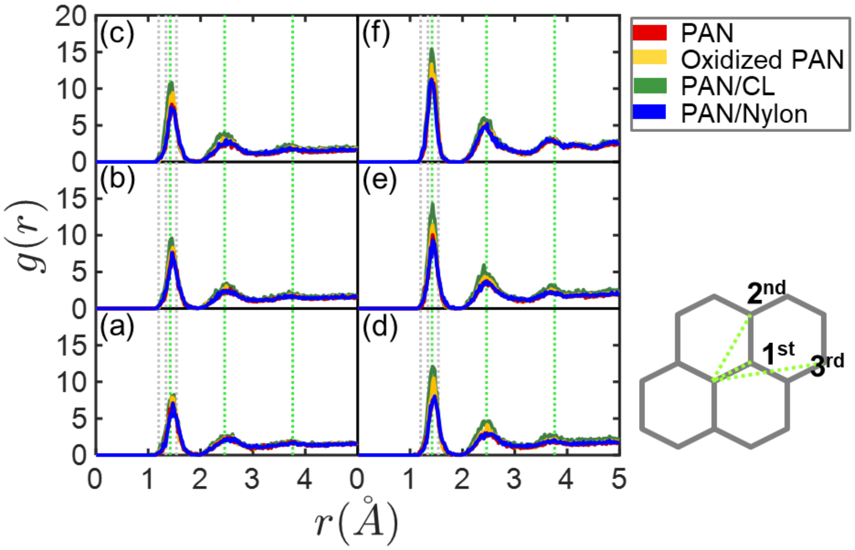

Figure S6. The RDF plots of PAN, oxidized PAN, PAN/CL, and PAN/Nylon carbonized at 2800K at (a) 250ps, (b) 450ps, (c) 750ps, (d) 1250ps, (f) 2250ps, and (e) 8250ps from ReaxFF MD simulations. The schematic shows the distances between the target C atom and its 1st, 2nd, and 3rd neighbor C atoms in a prefect graphene, which are 1.42Å, 2.46Å, and 3.76Å, respectively.

Table S2. The locations and intensities of the 1st peaks from RDF plots for PAN, oxidized PAN, PAN/CL, PAN/Nylon carbonized at 2800K at 250ps, 2250ps, and 8250ps from ReaxFF MD simulations; The I_D/I_G values from the Raman spectra for PAN, PAN/CL, and PAN/Nylon carbonized at 1500ºC from the experiment.

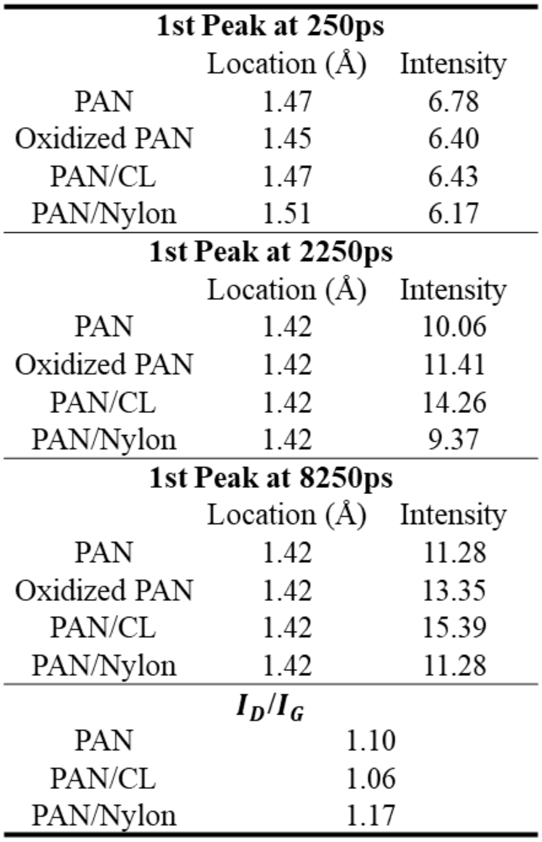

1st Peak at 250ps		
	Location (Å)	Intensity
PAN	1.47	6.78
Oxidized PAN	1.45	6.40
PAN/CL	1.47	6.43
PAN/Nylon	1.51	6.17
1st Peak at 2250ps		
	Location (Å)	Intensity
PAN	1.42	10.06
Oxidized PAN	1.42	11.41
PAN/CL	1.42	14.26
PAN/Nylon	1.42	9.37
1st Peak at 8250ps		
	Location (Å)	Intensity
PAN	1.42	11.28
Oxidized PAN	1.42	13.35
PAN/CL	1.42	15.39
PAN/Nylon	1.42	11.28
I_D/I_G		
PAN	1.10	
PAN/CL	1.06	
PAN/Nylon	1.17	

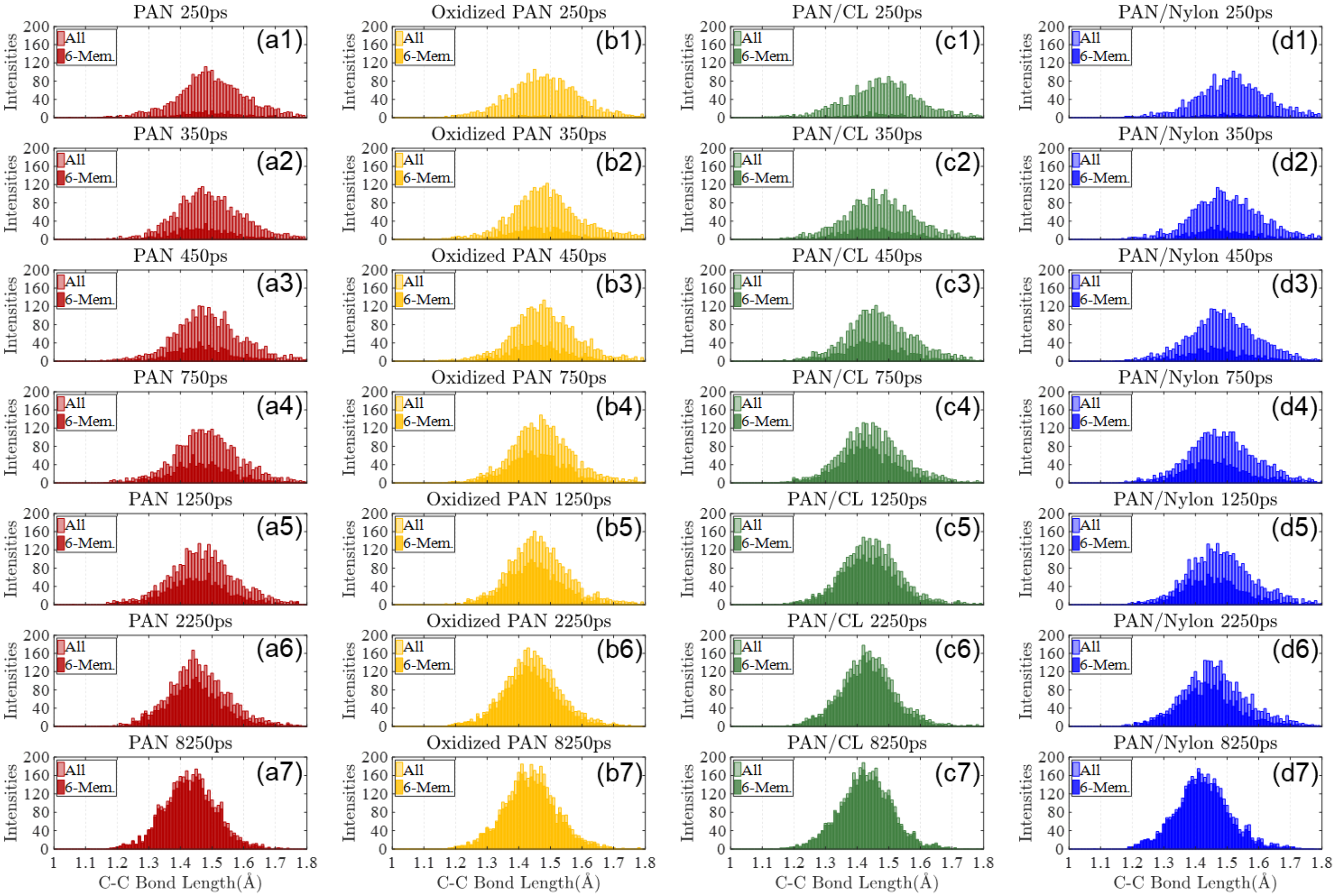

Figure S7. The C-C bond length distributions evolved over the carbonization time for the four representative precursors of interest: (a1-a7) PAN at 250ps, 350ps, 450ps, 750ps, 1250ps, 2250ps, and 8250ps, respectively; (b1-b7) Oxidized PAN at 250ps, 350ps, 450ps, 750ps, 1250ps, 2250ps, and 8250ps, respectively; (c1-c7) PAN/CL at 250ps, 350ps, 450ps, 750ps, 1250ps, 2250ps, and 8250ps, respectively; (d1-d7) PAN/CL at 250ps, 350ps, 450ps, 750ps, 1250ps, 2250ps, and 8250ps, respectively. The solid color distributions represent the C-C bonds forming the 6-membered all-carbon rings, and the transparent distributions represent the 3 to 8-membered all-carbon rings excluding the 6-membered all-carbon rings.